Iranian Journal of Medical Physics

ijmp.mums.ac.ir

A Follow-Up Study Investigating the Spectrum of Cognitive Impairment by MRI: Does Iron Cause Cognitive Dysfunction or Vice Versa?

Farzaneh Nikparast[1], Ali Shoeibi[2], Shabnam Niroumand[3], Hossein Akbari-Lalimi[1], Hoda Zare[1,4*]

1. Medical Physics Research Center, Mashhad University of Medical Sciences, Mashhad, Iran
2. Department of Neurology, Faculty of Medicine, Mashhad University of Medical Sciences, Mashhad, Iran
3. Department of Community Medicine, Faculty of Medicine, Mashhad University of Medical Sciences, Mashhad, Iran
4. Department of Medical Physics, Faculty of Medicine, Mashhad University of Medical Sciences, Mashhad, Iran

ARTICLE INFO

Article type:
Original Paper

Article history:
Received: Feb 19, 2023
Accepted: Aug 11, 2023

Keywords:
Cognitive Dysfunction
Neurodegenerative Diseases
Alzheimer Disease
Iron Metabolism Disorders

ABSTRACT

Introduction: Cognitive disorders, characterized by transient stages and potential Alzheimer's disease, are influenced by changes in iron deposits in the brain. These changes can lead to toxicity and neuron death. Quantitative susceptibility mapping is used to accurately represent these changes, allowing for a more accurate evaluation of the time window of each cognitive disorder stage and the need for targeted treatment.

Material and Methods: The Alzheimer's Disease Neuroimaging Initiative research database was used to download the data and eight healthy participants and twenty-one participants with cognitive disorders based on MMSE cognitive test scores in 5 groups of cognitively normal, Subjective Memory Concern , Early Mild Cognitive Impairment, Late Mild Cognitive Impairment and Alzheimer's disease were included in this study. Quantitative Susceptibility Mapping processing was performed using the SEPIA toolbox in MATLAB, and segmentation was performed using FSL software. Finally, statistical analyzes were performed using SPSS V26 software.

Results: Statistically significant changes were observed in the QSM values of the right thalamus (p-value = 0.043) in the LMCI group and the right hippocampal nucleus (p-value = 0.050) in the control group.

Conclusion: After one year, the right hippocampal nucleus shows increased iron accumulation in healthy individuals, suggesting that the nucleus is susceptible to the highest rate of iron deposition in healthy individuals. Based on this result, the hypothesis that iron deposits are the cause of the unknown cause-and-effect relationship between iron deposits and Alzheimer's disease may be confirmed.

► *Please cite this article as:*
Nikparast F, Shoeibi A, Niroumand Sh, Akbari-Lalimi H, Zare H. A Follow-Up Study Investigating The Spectrum Of Cognitive Impairment By MRI: Does Iron Cause Cognitive Dysfunction Or Vice Versa?. Iran J Med Phys 2024; 21: 194-202. 10.22038/IJMP.2023.70804.2248.

Introduction

Alzheimer's disease (AD) is a progressive and irreversible neurodegenerative disease with deficits in cognitive function and short-term memory[1].

According to the 2019 World Health Organization (WHO) report, AD is the seventh leading cause of death worldwide and imposes a high economic and social burden on society[2]. It is therefore necessary to detect these disorders early and before the onset of symptoms. Diagnosing this condition is challenging because some symptoms resemble the early stages of Alzheimer's disease and resemble the effects of normal aging. In general, the prevalence of this disorder increases with age, affecting approximately 50% of people over the age of 85 and 10% over the age of 65[3].

AD has also been observed in younger people around the age of 20 due to various factors such as genetic abnormalities. Mild cognitive impairment (MCI) is a transient stage in the aging process and is distinct from dementia, although it carries a high potential for developing Alzheimer's disease[4].

There are three grades of MCI based on the severity of the disorder, including Subjective Memory Concern (SMC), Early Mild Cognitive Impairment (EMCI) and Late Mild Cognitive Impairment(LMCI) [5].People in these stages suffer from some degree of cognitive impairment. Still, they don't have serious problems with everyday activities[6].

Cognitive deficits are more widespread across the spectrum of dementia disorders such as AD and significantly impair daily functioning. Brain changes during AD and MCI are generally classified into two morphologic and pathologic groups.

After clinical symptoms begin, the brain typically undergoes morphological or anatomical changes, including the atrophy of different areas of brain tissue[7-11]. The onset of clinical symptoms is preceded by pathologic changes, including deposits of

*Corresponding Author: Tel: +98-5138002321; Fax: +98-5138002320; Email: Zareh@mums.ac.ir

amyloid beta plaques, neurofibrillary tangles, and iron deposits[12-14].

Alzheimer's disease and MCI are characterized by the significant presence of iron in different regions of the brain, particularly the deep nuclei [15-17].

Its presence is necessary to carry out many natural and biological processes of the body, such as: Oxygen transport, cell cycle, gene expression, etc. Nevertheless, excessive iron deposition in the brain leads to cell damage and reduced brain functions through various processes; These processes are classified into two separate mechanisms.

In the first mechanism, which occurs under normal and disease-free conditions, iron produces reactive oxygen species and causes oxidative damage and cell death through ferroptosis[18, 19].

Under specific conditions, iron interacts with the markers of neurological diseases like amyloid beta plaques, alpha-synuclein granules, and tau protein, leading to their production and buildup in the body. The presence of iron in their structure enhances oxidative characteristics and results in the cell death[17].

Studies have shown that excessive iron deposition is associated with a variety of nervous system disorders such as Wilson's disease, Friedreich's ataxia (FA), major depression, amyotrophic lateral sclerosis (ALS), Parkinson's disease (PD), and Huntington's disease (HD)[20-25].

Histological studies indicate iron deposits in the brain areas of Alzheimer's patients; therefore, the hypothesis of a connection between iron metabolism and AD is proposed.

There are different techniques, such as Cerebrospinal fluid (CSF) sampling, blood biomarkers, and imaging methods based on Positron Emission Tomography (PET) and Magnetic Resonance Imaging (MRI) for early diagnosis of Alzheimer's disease; each technique has specific disadvantages, such as invasive performance, ionizing radiation, and high cost [26-29].

This article introduces the new and non-invasive Quantitative Susceptibility Mapping (QSM) technique, a type of post-processing of MRI imaging [30].

The aim of this research project is to evaluate changes in the QSM values of brain nuclei after one year; The results would determine the importance of timely initiation of clinical procedures at each stage of MCI.

Materials and Methods

Database

Images obtained from MRI scans in two sets of T1-weighted structure and multi-echo GRE (magnitude and phase images separately). This data was downloaded from the Alzheimer's Disease Neuroimaging Initiative (ADNI) research database[31].

Participants

The criteria for selecting subjects include

a) The five groups individuals should belong to are CN, SMC, EMCI, LMCI, and AD.; b) The scans of these individuals should include both multi-echo GRE and T1W.c) Separate phase and magnitude images should be provided.; d, There should be access to data on cognitive information, including MMSE scores. According to the purpose of this research, which is to study the changes in iron deposits in the brain nuclei of the studied groups, the participants were selected based on the test results of the Mini-Mental State Examination (MMSE).

Therefore, eight healthy participants as a control group and twenty-one participants with cognitive disorders were included in this study (Table 1).

After a period of 12 ± 5.6 months, the subjects of each group underwent an MRI scan again with the initial parameters.

Table 1.Analysis of the demographic information of the participants

Characteristic	CN (8)	SMC (4)	EMCI (5)	LMCI (7)	AD (5)	P-Value
Age1 (Mean±SD)	80.875±6.770	78.000±4.690	78.400±4.827	76.857±5.429	81.600±4.159	0.52
Age2 (Mean±SD)	81.875±6.770	79.000±4.690	80.000±5.354	77.857±5.429	82.600±4.159	0.52
MMSE Score1 (Mean±SD)	28.625±1.685	28.250±1.500	26.800±2.387	26.714±3.988	23.400±4.449	0.62
MMSE Score2 (Mean±SD)	28.250±1.669	26.500±2.886	26.000±5.228	26.857±3.532	16.400±7.266	<0.001
Sex	5 Female and 3 Male	2 Female and 2 Male	1 Female and 4 Male	2 Female and 5 Male	2 Female and 3 Male	0.35

* CN, cognitively normal; SMC, subjective memory concerns; EMCI, early mild cognitive impairment; LMCI, late mild cognitive impairment; AD, Alzheimer's disease; MMSE, Mini-Mental State Examination.
P ≤ 0.05 was considered statistically significant and bold font indicates statistical significance.
Age1, Age of the participant in the first brain scan; Age2,Age of the participant in the second brain scan.

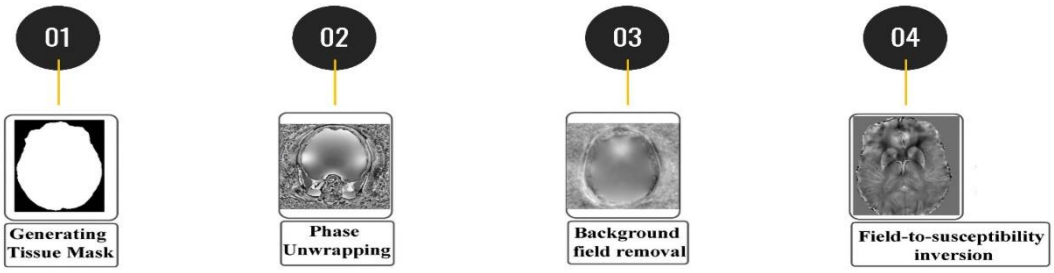

Figure 1. QSM Reconstruction Step.
Generating Tissue Mask, Phase Unwrapping, Background Field Removal and Field-to-susceptibility inversion

MRI Acquisition

A Siemens 3 Tesla prism scanner with neck coils was used for the scans.The 3D Accelerated_Sagittal_MPRAGE sequence was implemented as a structural and anatomical image and the parameters include:

acquisition matrix and reconstruction matrix = 240, pixel bandwidth = 240, flip angle = 9, slice thickness (mm) = 1, TE/TI (ms) = 2.98/900,and TR (ms) = 2300.

The multi-echo GRE sequence required for the QSM reconstruction is implemented using these parameters: number of slices=44, voxel size y and x (mm) = 0.859375 (mm) = 0.859375, matrix size = 256256, pixel bandwidth = 260, flip angle = 20, slice thickness (mm) = 4, TE1-TE2-TE3 (ms) = 6.09-13-20, and TR (ms) = 650.

Image Processing

Quantitative Susceptibility Mapping

Phase and magnitude image processing was done with the SEPIA toolbox and MATLAB[32, 33].

Using the Brain Extraction Tool (BET) toolbox, the brain mask was extracted from magnitude images and used to combine with the final QSM image[34].

To create the reconstructed QSM image, three stages of phase unwrapping, background field removal, and dipole inversion were applied to the phase images. To avoid the occurrence of aliasing artifacts and to correctly estimate the magnetic susceptibility of the tissue, phase unwrapping was performed using the Laplace tool available in the STI Suite[35].

The background field removal stage aims to remove the unwanted background of magnetic susceptibility changes in phase images; The V-SHARP toolbox in the STI suite was used for this purpose. Finally, the QSM image was reconstructed in ppm using the STAR algorithm.

Automatic Segmentation

In the last step, the anatomical field of the brain nuclei needed to be determined; for this purpose, the FIRST tool available in the FSL software was used to segment automatically

(https://fsl.fmrib.ox.ac.uk/fsl/fslwiki/FIRST).

The location of twelve nuclei was determined, including left-thalamus, left-caudate, left-putamen, left-pallidum, left-Hippocampus, left-amygdala, right-Thalamus, right-caudate, right-putamen, right-pallidum, right-hippocampus, and right-amygdala.

The segmented brain nuclei were evaluated by a neurologist and after confirming the correctness of contouring ROIs, statistical analyzes were started.

To measure the mean QSM values of brain nuclei, QSM segments and images were entered as input to the 3D slicer software[36].Finally, statistical analyzes were performed using SPSS version 26 software (Figure 1).

Statistical analysis

Demographic information on age and MMSE scores were evaluated using ANOVA test and gender data using chi-square test. Due to the limited number of participants in this study, the Shapiro-Wilk test was used to assess the normality of these data. The differences in magnetic susceptibility of the specific brain nuclei in the groups under study were evaluated using comparative tests during the time period between two scans. (mean = 12 months, SD = 5.6 months). Paired-samples t-test was used for normally distributed variables and the Wilcoxon Signed Ranks test was used for non-normally distributed variables.

Results

A time-longitudinal study was performed to examine changes in the magnetic susceptibility of brain nuclei in each patient group. Eight CN, four SMC, five EMCI, seven LMCI, and five AD participants were included in this study.

Demographic information on quantitative variables was evaluated using the one-way ANOVA test, and gender-related data were evaluated using the chi-square test. Based on the results, only the MMSE variable at the time of the patients' second scan showed a significant difference between the studied groups ($P<0.001$), while the other variables showed no significant difference between the studied groups (Table1).

Based on the results of the Shapiro-Wilk test, an abnormal distribution was observed in the data on the left putamen, left amygdala, right putamen, right thalamus, and right hippocampus nuclei (Table2).

The magnetic susceptibility of each brain nucleus in the studied groups was compared using comparative tests during the time interval between two scans. (mean = 12 months, SD = 5.6 months). The paired-samples t-test was used when variables were normally distributed, and the

Wilcoxon Signed Ranks test was used when the distribution was nonnormal (Tables 3, 4, sup1 and sup2).

The results showed statistically significant changes in the QSM values of the two right thalamic nuclei (p-value=0.043) in the LMCI group and the right hippocampal nucleus (p-value=0.050) in the control group. Thus, the magnetic susceptibility of the right thalamic nucleus in the LMCI group decreases over time and the right hippocampal nucleus in the control group increases over time.

Table 2 .Examining the normal distribution of QSM data of brain nuclei (Shapiro-Wilk test): (A: First scan, B: Second scan)

		Shapiro-Wilk Test				
		CN	SMC	EMCI	LMCI	AD
A	Left Thalamus1	0.541	0.174	0.729	0.601	0.314
	Left Caudate1	0.778	0.103	0.475	0.358	0.236
	Left Putamen1	0.017	0.883	0.842	0.368	0.903
	Left Pallidum1	0.542	0.480	0.430	0.063	0.933
	Left Hippocampus 1	0.580	0.396	0.551	0.028	0.348
	Left Amygdala1	0.661	0.033	0.360	0.984	0.943
	Right Thalamus1	0.735	0.271	0.608	0.818	0.592
	Right Caudate1	0.863	0.268	0.384	0.735	0.292
	Right Putamen1	0.084	0.956	0.952	0.019	0.307
	Right Pallidum1	0.258	0.956	0.251	0.053	0.973
	Right Hippocampus1	0.100	0.493	0.451	0.888	0.187
	Right Amygdala1	0.053	0.985	0.085	0.846	0.119
B	Left Thalamus2	0.314	0.051	0.214	0.865	0.592
	Left Caudate2	0.070	0.981	0.077	0.520	0.845
	Left Putamen2	0.149	0.076	0.774	0.058	0.739
	Left Pallidum2	0.340	0.584	0.157	0.995	0.801
	Left Hippocampus2	0.476	0.236	0.539	0.963	0.665
	Left Amygdala2	0.017	0.949	0.239	0.190	0.691
	Right Thalamus2	0.765	0.705	0.140	0.314	0.033
	Right Caudate2	0.720	0.425	0.665	0.316	0.888
	Right Putamen2	0.511	0.975	0.462	0.302	0.047
	Right Pallidum2	0.970	0.958	0.395	0.105	0.952
	Right Hippocampus2	0.993	0.306	0.454	0.002	0.486
	Right Amygdala2	0.748	0.040	0.036	0.246	0.035

P ≤ 0.05 was considered statistically significant and bold font indicates statistical significance. CN: cognitively normal, SMC: subjective memory concerns, EMCI: early mild cognitive impairment, LMCI: late mild cognitive impairment, AD: Alzheimer's disease;

Table 3. Examining changes in the magnetic susceptibility of the brain nuclei after one year (Wilcoxon Signed Ranks Test)

	Wilcoxon Signed Ranks Test				
	CN	SMC	EMCI	LMCI	AD
Left Putamen1 vs. Left Putamen2	0.575	0.068	0.225	0.310	0.686
Left Amygdala1 vs. Left Amygdala2	0.575	0.465	0.686	0.612	0.345
Right Thalamus 1 vs. Right Thalamus2	0.327	0.273	0.715	0.043*	0.500
Right Putamen 1 vs. Right Putamen2	0.401	0.465	0.345	0.176	0.686
Right Hippocampus1 vs. Right Hippocampus2	0.050*	0.465	0.686	0.612	0.138
Right Amygdala 1 vs. Right Amygdala2	0.327	0.068	0.893	0.499	0.500

P ≤ 0.05 was considered statistically significant and bold font indicates statistical significance. CN: cognitively normal, SMC: subjective memory concerns, EMCI: early mild cognitive impairment, LMCI: late mild cognitive impairment, AD: Alzheimer's disease;

Table 4. Examining changes in the magnetic susceptibility of the brain nuclei after one year, (Paired samples Test)

	Paired Samples Test				
	CN	SMC	EMCI	LMCI	AD
Left Thalamus 1 vs. Left Thalamus2	0.618	0.863	0.783	0.352	0.149
Left Caudate 1 vs. Left Caudate2	0.726	0.623	0.544	0.674	0.187
Left Pallidum 1 vs. Left Pallidum2	0.755	0.385	0.553	0.554	0.784
Left Hippocampus 1 vs. Left Hippocampus2	0.523	0.470	0.992	0.351	0.058
Right Pallidum 1 vs. Right Pallidum2	0.281	0.995	0.211	0.985	0.468

$P \leq 0.05$ was considered statistically significant and bold font indicates statistical significance. CN: cognitively normal, SMC: subjective memory concerns, EMCI: early mild cognitive impairment, LMCI: late mild cognitive impairment, AD: Alzheimer's disease.

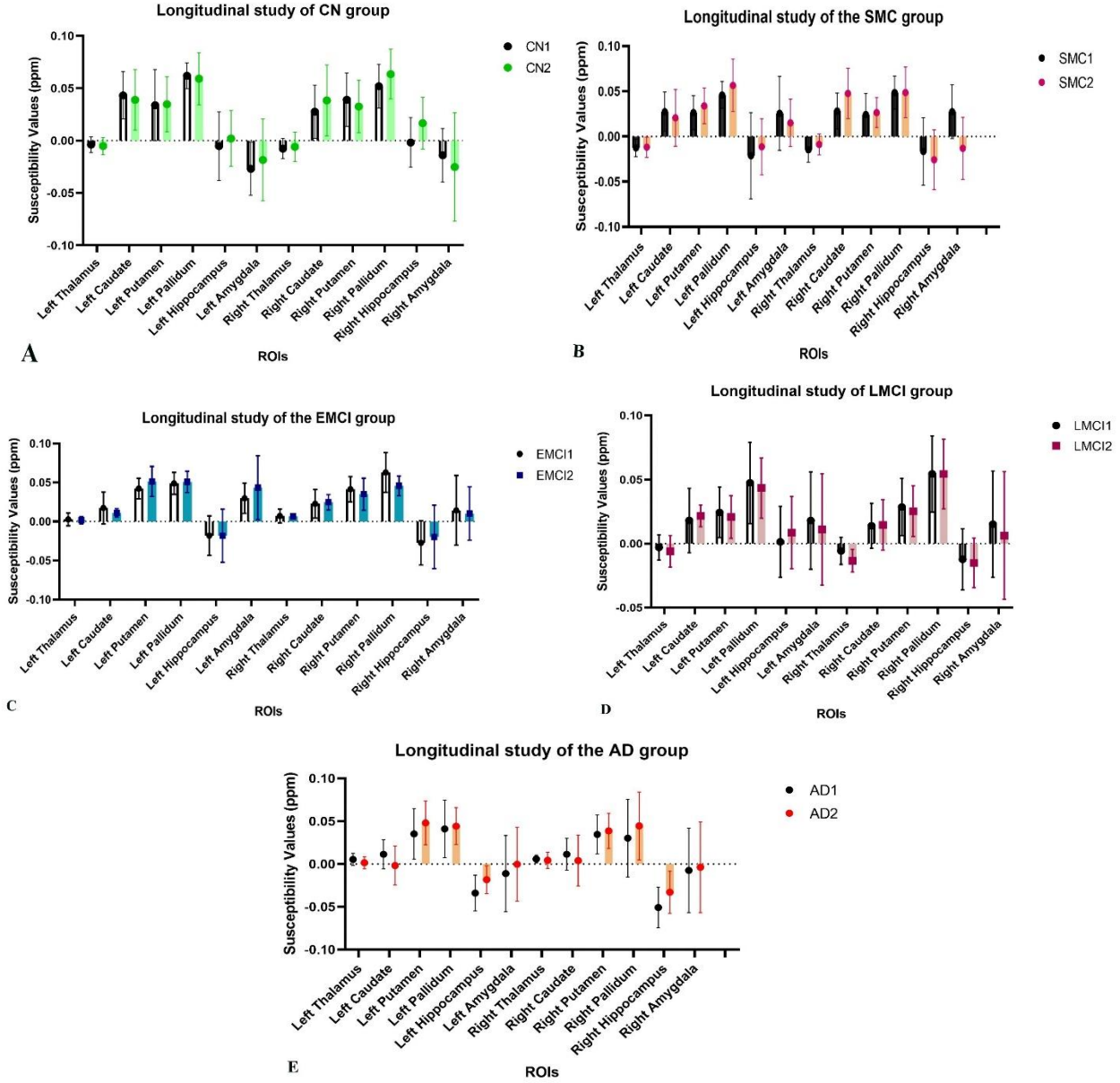

Figure 2. Mean QSM values of brain nuclei of the studied groups. The numbers 1 and 2 after the abbreviation of the name of each participant group (CN, SMC, EMCI, LMCI and AD) mean the first scan and the second MRI scan at 12 5.6 months. CN, cognitively normal; SMC, subjective memory concerns; EMCI, early mild cognitive impairment; LMCI, late mild cognitive impairment; AD, Alzheimer's disease. $P \leq 0.05$ was considered statistically significant and bold font indicates statistical significance.

Discussion

Microscopic or pathological changes in the deep brain nuclei include iron deposits and amyloid beta plaques, which precede morphological changes like atrophy in different brain regions. However, the lack of dependable and sensitive biomarkers for these pathological changes means that diagnosis in advanced disease stages primarily relies on clinical observations.

In this research, upon introduction of the new QSM technique, the rate of changes in iron deposition in the brain nuclei of each group of participants was measured to identify a stage of cognitive impairment with the most changes at one year. The basis of this new technique is based on the magnetic susceptibility of tissue; This feature is a physical response of the tissue to the application of the external magnetic field, which reflects the tissue's contents.

Iron is a paramagnetic material; This leads to positive changes in the magnetic susceptibility of tissues.

The human body relies heavily on iron, making it the most important rare element. Iron plays an important role in body functions such as neurotransmitter synthesis, brain growth and physiology, mitochondrial reactions and cytoplasmic protein function. The main source of iron in the central nervous system is non-transferrin-bound iron (NTBI). In addition, DMT1 is an important transporter in the body that helps with iron absorption. When this iron transporter malfunctions, excess iron is deposited in the brain, leading to neurotoxicity and significant cognitive impairment. Ferroptosis is an iron-dependent cell death process and is usually associated with lipid peroxidation. A close connection between ferroptosis and other pathophysiological processes of many diseases has been observed in various studies [37-41]. Several in vitro studies have confirmed the effect of iron deposition on neuronal death. A recent in vitro study showed that the use of ferrostatin-1, a selective inhibitor of ferroptosis, preserves mitochondrial function and reduces neuronal cell death[42, 43]

Iron builds up over time in various brain structures, including the deep nuclei, hippocampus, cerebellum, and subcortical areas, with the highest levels found in the deep gray matter (DGM). Ayton et al.'s research demonstrates a significant link between iron accumulation in the inferior temporal gyrus (ITG) and cognitive decline in individuals with Aβ plaques, tau protein, and neurofibrillary tangles. In essence, the increase in iron concentration creates favorable conditions for amyloid beta accumulation and the onset of neurotoxicity[44].

The link between iron buildup and neurological diseases remains uncertain despite extensive research in this area. Nonetheless, analyzing the location and quantity of iron accumulation can enhance our comprehension of the progression of cognitive disorders and the sequence of pathological occurrences.

According to the results, the amount of iron deposition in the LMCI and control groups has the highest rate of change, so the magnetic susceptibility of the right thalamic nucleus in the LMCI group decreases over time and that of the right hippocampal nucleus in the control group increases (**Figure 2**).

The decrease in the paramagnetic properties of the right thalamus nucleus in the LMCI group over a year may indicate the occurrence of the plateau effect, the deposition of other diamagnetic substances, or some kind of compensatory response in advanced stages of cognitive disorders, which requires further research in this area.

A one-year longitudinal study in the group of participants with cognitive disorders has not yet been carried out.

In the longitudinal study conducted in 2020 by Fan et al. on three groups of AD, MCI and control, No significant difference was observed in the brain and cerebellar nuclei after six months[45].

Comparative studies between normal and abnormal cognitive groups have been widely conducted.

In three studies by Kim et al. ,Li et al. and Kan et al. hippocampal nucleus QSM values of the AD group were significantly higher than those of the control group, consistent with the results of our research[46-48].

The QSM values of the right hippocampal nucleus in the group of normal people increase over the course of a year, indicating the susceptibility of this nucleus to iron deposits.

The hippocampus, situated in the limbic system, is vital for regulating emotions and responses and is pivotal for memory and learning processes. Unfortunately, it is impacted by Alzheimer's disease, along with other brain regions. Found in the depths of the temporal lobe, this structure is responsible for converting short-term memories into long-term ones.

Numerous research studies have documented the rapid decline in hippocampal volume during the early stages of Alzheimer's disease, along with the disruption of functional connections to other brain regions. The hippocampus plays a crucial role in processing and recalling two distinct types of memories: declarative memory, which encompasses facts and events, and spatial memory, which involves remembering spatial relationships.

Declarative memories pertain to factual information and past events, such as memorizing words or passages from a book. Spatial memory, on the other hand, involves recalling spatial relationships and layouts, such as navigating a city's streets, which taxi drivers often rely on. It appears that spatial memory is primarily stored in the right hippocampus.

The hippocampus is responsible for converting short-term memories into long-term memories and then storing them in another area of the brain. If diseases like Alzheimer's damage one or both parts of the hippocampus, an individual may experience memory loss and difficulty in forming new, enduring memories.

Alternatively, it is possible to forget some new memories while remembering old ones; This is because long-term memories, once they have become longer-

term, are stored in another part of the brain and are not affected by damage to the hippocampus. According to the finding, cognitive disorders first affect the hippocampus; Short-term memory loss is one of the early symptoms of the disease.

As the illness advances, the hippocampus experiences a substantial decrease in size, which can hinder the individual's ability to perform everyday activities. There seems to be a connection between Alzheimer's disease and depression and the shrinking of the hippocampus. Thus, in Alzheimer's disease, assessing the hippocampus's dimensions can be utilized to gauge the progression of the illness.

The most critical limitations were the small size of the statistical population of subjects studied. The unavailability of a suitable strength (3 Tesla) MRI scanner at the research center and the inability to collect suitable images (phase and magnitude separately) are the reasons for using the ADNI database.

Another limitation is the statistical difference in the sex variable of the groups studied. Conducting this research with a larger sample size can complement this study so that the results obtained have enough credibility to cite. Examining the compatibility of QSM reconstruction results with PET images will be a practical step in evaluating the clinical performance of this technique.

It is also proposed to evaluate the performance of the QSM technique in other neurodegenerative diseases such as Parkinson's, autism, Huntington's disease, depression, MS, AIDS-related cognitive disorders, Covid-19-related cognitive disorders and anxiety. The comparison of different algorithms of the QSM reconstruction steps can also complement this research project.

Conclusion

After one year, the right hippocampal nucleus shows increased iron accumulation in healthy people, suggesting that the nucleus is prone to the highest rate of iron deposition in healthy people. Based on this result, the hypothesis that iron deposits are the cause of the unknown cause-and-effect relationship between iron deposits and Alzheimer's disease may be confirmed. However, the right thalamic nucleus in the LMCI group shows a decrease in QSM values, which may be due to various reasons, such as the appearance of the plateau effect, the compensation mechanism, or the deposition of other diamagnetic substances.

Acknowledgment

Data collection and sharing for this project was funded by the Alzheimer's Disease Neuroimaging Initiative (ADNI) (National Institutes of Health Grant U01 AG024904) and DOD ADNI (Department of Defense award number W81XWH-12-2-0012). The authors would like to express their gratitude to Mashhad University of Medical Sciences for the financial support of this thesis, with the following code of ethics: IR.MUMS.MEDICAL.REC.1400.510. The online version of the approval is available at the following address and is open to the public: https://ethics.research.ac.ir/IR.MUMS.MEDICAL.REC.1400.510

References

1. O'Bryant SE, Mielke MM, Rissman RA, Lista S, Vanderstichele H, Zetterberg H, et al. Blood-based biomarkers in Alzheimer disease: current state of the science and a novel collaborative paradigm for advancing from discovery to clinic. Alzheimer's & Dementia. 2017;13(1):45-58.
2. 2022 Alzheimer's disease facts and figures. Alzheimer's & Dementia. 2022;18(4):700-89.
3. Pais R, Ruano L, Moreira C, Carvalho OP, Barros H. Prevalence and incidence of cognitive impairment in an elder Portuguese population (65–85 years old). BMC Geriatrics. 2020;20(1):470.
4. Pandya SY, Clem MA, Silva LM, Woon FL. Does mild cognitive impairment always lead to dementia? A review. Journal of the neurological sciences. 2016;369:57-62.
5. Sanford AM. Mild cognitive impairment. Clinics in geriatric medicine. 2017;33(3):325-37.
6. Jessen F, Wolfsgruber S, Wiese B, Bickel H, Mösch E, Kaduszkiewicz H, et al. AD dementia risk in late MCI, in early MCI, and in subjective memory impairment. Alzheimer's & Dementia. 2014;10(1):76-83.
7. Gong N-J, Chan C-C, Leung L-M, Wong C-S, Dibb R, Liu C. Differential microstructural and morphological abnormalities in mild cognitive impairment and Alzheimer's disease: Evidence from cortical and deep gray matter. Human brain mapping. 2017;38(5):2495-508.
8. Khadem-Reza ZK, Zare H. Evaluation of brain structure abnormalities in children with autism spectrum disorder (ASD) using structural magnetic resonance imaging. The Egyptian Journal of Neurology, Psychiatry and Neurosurgery. 2022;58(1):135.
9. Nikparast F, Shoeibi A, Niroumand S, Akbari-Lalimi H, Zare H. Application of Nobel QSM technique in MRI for diagnosis of Alzheimer's disease: What is the relationship between iron deposits in brain nuclei with age and severity of disorders? Medical Journal of Tabriz University of Medical Sciences. 2023;45(2):130-40.
10. Faraji R, Ganji Z, Zamanpour SA, Nikparast F, Akbari-Lalimi H, Zare H. Impaired white matter integrity in infants and young children with autism spectrum disorder: What evidence does diffusion tensor imaging provide? Psychiatry Research: Neuroimaging. 2023:111711.
11. Nikparast F, Shoeibi A, Niroumand S, Akbari-Lalimi H, Zare H. Brain Nucleus Changes in Cognitive Disorders: Examining By the Quantitative Susceptibility Mapping (QSM) Technique. Iranian Journal of Medical Physics/Majallah-I Fīzīk-I Pizishkī-i Īrān. 2024;21(1).
12. Palop JJ, Mucke L. Amyloid-β–induced neuronal dysfunction in Alzheimer's disease: from synapses toward neural networks. Nature neuroscience. 2010;13(7):812-8.

13. Lin MT, Beal MF. Mitochondrial dysfunction and oxidative stress in neurodegenerative diseases. Nature. 2006;443(7113):787-95.
14. Mesulam M. The cholinergic lesion of Alzheimer's disease: pivotal factor or side show? Learning & memory. 2004;11(1):43-9.
15. Nikparast F, Ganji Z, Danesh Doust M, Faraji R, Zare H. Brain pathological changes during neurodegenerative diseases and their identification methods: How does QSM perform in detecting this process? Insights into Imaging. 2022;13(1):74.
16. Nikparast F, Ganji Z, Zare H. Early differentiation of neurodegenerative diseases using the novel QSM technique: what is the biomarker of each disorder? BMC Neurosci. 2022;23(1):48.
17. Morris G, Berk M, Carvalho AF, Maes M, Walker AJ, Puri BK. Why should neuroscientists worry about iron? The emerging role of ferroptosis in the pathophysiology of neuroprogressive diseases. Behavioural brain research. 2018;341:154-75.
18. Ndayisaba A, Kaindlstorfer C, Wenning GK. Iron in neurodegeneration−cause or consequence? Frontiers in neuroscience. 2019;13:180.
19. Dixon SJ, Lemberg KM, Lamprecht MR, Skouta R, Zaitsev EM, Gleason CE, et al. Ferroptosis: an iron-dependent form of nonapoptotic cell death. Cell. 2012;149(5):1060-72.
20. Van Bergen JM, Hua J, Unschuld PG, Lim IAL, Jones CK, Margolis RL, et al. Quantitative susceptibility mapping suggests altered brain iron in premanifest Huntington disease. American journal of neuroradiology. 2016;37(5):789-96.
21. Fritzsch D, Reiss-Zimmermann M, Trampel R, Turner R, Hoffmann K-T, Schäfer A. Seven-tesla magnetic resonance imaging in Wilson disease using quantitative susceptibility mapping for measurement of copper accumulation. Investigative radiology. 2014;49(5):299-306.
22. Doganay S, Gumus K, Koc G, Bayram AK, Dogan MS, Arslan D, et al. Magnetic susceptibility changes in the basal ganglia and brain stem of patients with Wilson′s disease: evaluation with quantitative susceptibility mapping. Magnetic Resonance in Medical Sciences. 2018;17(1):73.
23. Kwan JY, Jeong SY, Van Gelderen P, Deng H-X, Quezado MM, Danielian LE, et al. Iron accumulation in deep cortical layers accounts for MRI signal abnormalities in ALS: correlating 7 tesla MRI and pathology. PloS one. 2012;7(4):e35241.
24. Schweitzer AD, Liu T, Gupta A, Zheng K, Seedial S, Shtilbans A, et al. Quantitative susceptibility mapping of the motor cortex in amyotrophic lateral sclerosis and primary lateral sclerosis. AJR American journal of roentgenology. 2015;204(5):1086.
25. La Rosa P, Petrillo S, Fiorenza MT, Bertini ES, Piemonte F. Ferroptosis in Friedreich′s Ataxia: A Metal-Induced Neurodegenerative Disease. Biomolecules. 2020;10(11):1551.
26. Li J, Chang S, Liu T, Wang Q, Cui D, Chen X, et al. Reducing the object orientation dependence of susceptibility effects in gradient echo MRI through quantitative susceptibility mapping. Magnetic resonance in medicine. 2012;68(5):1563-9.
27. Haacke EM, Xu Y, Cheng YC, Reichenbach JR. Susceptibility weighted imaging (SWI). Magnetic resonance in medicine. 2004;52(3):612-8.
28. Walsh AJ, Wilman AH. Susceptibility phase imaging with comparison to R2 mapping of iron-rich deep grey matter. NeuroImage. 2011;57(2):452-61.
29. Meadowcroft MD, Connor JR, Smith MB, Yang QX. MRI and histological analysis of beta-amyloid plaques in both human Alzheimer's disease and APP/PS1 transgenic mice. Journal of Magnetic Resonance Imaging: An Official Journal of the International Society for Magnetic Resonance in Medicine. 2009;29(5):997-1007.
30. Haacke EM, Liu S, Buch S, Zheng W, Wu D, Ye Y. Quantitative susceptibility mapping: current status and future directions. Magnetic resonance imaging. 2015;33(1):1-25.
31. ADNI [Internet]. 2003. Available from: https://adni.loni.usc.edu/.
32. Feng X, Deistung A, Reichenbach JR. Quantitative susceptibility mapping (QSM) and R2* in the human brain at 3 T: Evaluation of intra-scanner repeatability. Zeitschrift für Medizinische Physik. 2018;28(1):36-48.
33. Chan K-S, Marques JP. SEPIA—susceptibility mapping pipeline tool for phase images. NeuroImage. 2021;227:117611.
34. Straub S, Schneider TM, Emmerich J, Freitag MT, Ziener CH, Schlemmer HP, et al. Suitable reference tissues for quantitative susceptibility mapping of the brain. Magnetic resonance in medicine. 2017;78(1):204-14.
35. Li W, Wu B, Liu C. Quantitative susceptibility mapping of human brain reflects spatial variation in tissue composition. NeuroImage. 2011;55(4):1645-56.
36. Fedorov A, Beichel R, Kalpathy-Cramer J, Finet J, Fillion-Robin J-C, Pujol S, et al. 3D Slicer as an image computing platform for the Quantitative Imaging Network. Magnetic resonance imaging. 2012;30(9):1323-41.
37. Singh N, Haldar S, Tripathi AK, Horback K, Wong J, Sharma D, et al. Brain iron homeostasis: from molecular mechanisms to clinical significance and therapeutic opportunities. Antioxidants & redox signaling. 2014;20(8):1324-63.
38. Codazzi F, Pelizzoni I, Zacchetti D, Grohovaz F. Iron entry in neurons and astrocytes: a link with synaptic activity. Frontiers in molecular neuroscience. 2015;8:18.
39. Knutson MD. Non-transferrin-bound iron transporters. Free Radical Biology and Medicine. 2019;133:101-11.
40. Wang Z, Zeng Y-N, Yang P, Jin L-Q, Xiong W-C, Zhu M-Z, et al. Axonal iron transport in the brain modulates anxiety-related behaviors. Nature chemical biology. 2019;15(12):1214-22.
41. Mills E, Dong XP, Wang F, Xu H. Mechanisms of brain iron transport: insight into neurodegeneration and CNS disorders. Future medicinal chemistry. 2010;2(1):51-64.
42. Xia Y, Sun X, Luo Y, Stary CM. Ferroptosis contributes to isoflurane neurotoxicity. Frontiers in Molecular Neuroscience. 2019;11:486.
43. Li J, Cao F, Yin H-l, Huang Z-j, Lin Z-t, Mao N, et al. Ferroptosis: past, present and future. Cell death & disease. 2020;11(2):88.

44. Ayton S, Wang Y, Diouf I, Schneider JA, Brockman J, Morris MC, et al. Brain iron is associated with accelerated cognitive decline in people with Alzheimer pathology. Molecular psychiatry. 2020;25(11):2932-41.
45. Fan X, Liu X, Yan L, Mok VCT, Li K. Assessment of brain iron accumulation in Alzheimer's disease with quantitative susceptibility mapping. Alzheimer's & Dementia. 2020;16(S4):e038799.
46. Kim HG, Park S, Rhee HY, Lee KM, Ryu CW, Rhee SJ, et al. Quantitative susceptibility mapping to evaluate the early stage of Alzheimer's disease. NeuroImage Clinical. 2017;16:429-38.
47. Li DT, Hui ES, Chan Q, Yao N, Chua S, McAlonan GM, et al. Quantitative susceptibility mapping as an indicator of subcortical and limbic iron abnormality in Parkinson's disease with dementia. NeuroImage: Clinical. 2018;20:365-73.
48. Kan H, Uchida Y, Arai N, Ueki Y, Aoki T, Kasai H, et al. Simultaneous voxel-based magnetic susceptibility and morphometry analysis using magnetization-prepared spoiled turbo multiple gradient echo. NMR in biomedicine. 2020;33(5):e4272.